Auto-Optimization of Dewetting Rates by Rim Instabilities in Slipping Polymer Films

Günter Reiter
Institut de Chimie des Surfaces et Interfaces, CNRS, 15, rue Jean Starcky, B.P. 2488, 68057 Mulhouse Cedex, France

Ashutosh Sharma
Department of Chemical Engineering, Indian Institute of Technology at Kanpur, India 208 016
(Received 4 December 2000; published 1 October 2001)

We investigated the instability of the moving rim in dewetting of slipping polymer films. Small fluctuations of the width of the rim get spontaneously amplified since narrower sections of the rim move faster than wider ones due to frictional forces being proportional to the width of the rim. Instability leads eventually to an autocontrol of the rim width by the continuous formation of droplets with a mean size proportional to the initial film thickness. Surprisingly, the mean dewetting velocity at late stages, averaged over the length of the rim, was found to be constant. Thus, the instability of the rim enabled a more efficient, i.e., faster, "drying" of the substrate. Nonslipping films did not show this instability.

DOI: 10.1103/PhysRevLett.87.166103 PACS numbers: 68.03.Cd, 61.41.+e, 68.08.Bc, 68.15.+e

Retraction of a liquid from a nonwettable solid substrate is a process frequently encountered in nature and technology. Many fundamental studies of such dewetting processes were done with spin coated thin polymer films (e.g., [1,2]). Usually the removed liquid is collected in a rim. Already in earlier dewetting experiments [2–4] instabilities of the rim similar to fingers were observed. In the majority of experiments, however, no such instabilities were seen [2,5–10]. The rim instabilities during dewetting suggest some relation to the Rayleigh instability of an immobile liquid ridge in that no external forces are responsible for the instability [3]. This is in contrast to the fingering instabilities observed under the influence of centrifugal forces [11], thermal [12–15], or concentration gradients [16]. Some similarities to rim instabilities in dewetting of highly volatile liquids [17] and fingering in elastic films [18,19] also exist. There is as yet no clear understanding of why such instabilities occur in dewetting films and why, on the contrary, in many cases the retracting rim appears to be stable.

The velocity of an intrinsic dewetting process (not driven by the application of external forces) is set by the balance of capillary driving forces and viscous dissipation forces [1,20,21]. While the capillary forces depend mostly on static properties and are thus time independent, dissipation may vary with time, e.g., if the frictional forces are proportional to the size of the moving liquid body, as it is the case when the liquid "slips" on top of the substrate [20,21]. It has been shown in previous experiments [22] that in autophobic polymer dewetting, where a thin film of polymer melt dewets a densely end-grafted layer of identical polymers, the dewetting velocity decreases with the size of the rim collecting the liquid from the already dewetted area. Based on these considerations an intriguing question arises. What happens if for some reason the width of the rim starts to fluctuate along its length? Then, there are thinner parts which resist less to the driving capillary forces and thicker ones which are moving slower. This question is addressed in the present study.

For our experiments we used, as in previous studies [22–25], thin polydimethylsiloxane (PDMS) films [molecular weight $M_w = 308$ kg/mol, viscosity η (25 °C) = 1000 Pa · s or, alternatively, $M_w = 156$ kg/mol, η (25 °C) = 100 Pa · s] of different thicknesses between 10 and 100 nm (as measured by ellipsometry) on top of silicon substrates coated with densely grafted layers (polymer brushes) of end-functionalized PDMS molecules ($M_w = 8.8$ kg/mol, index of polydispersity $I_p = 1.07$) or layers of adsorbed PDMS ($M_w = 38.3$ kg/mol, $I_p = 2.56$). We used many different samples with about the same thickness m of the monolayer: $m = 6 \pm 1$ nm. The grafting density Σ is implicitly given: $\Sigma = m/$volume of a polymer chain. The adsorbed layers resulted from annealing spin coated films on hydroxylated (UV-ozone treated) silicon wafers at 150 °C for 5 h under vacuum [25]. Layers of strongly adsorbed or densely grafted polymers showed autophobic behavior and were stable under the conditions of our experiments [22,23,26]. All films deposited on top of these monolayers were metastable and started to dewet at a straight three-phase contact line which was created by breaking the silicon substrate along a crystallographic axis in two parts [22]. Dewetting was followed in real time by optical microscopy at temperatures between room temperature and 130 °C. Further details about experimental procedures, aspects related to sample preparation, and data analysis can be found in [22,23,25].

In Fig. 1 we present typical results showing the differences between dewetting on an adsorbed and on a grafted PDMS layer. On the adsorbed layer (Figs. 1A–1D) the moving rim grew only in width — reflecting the increasing volume of the melt from the dewetted area — without clear signs of instabilities. The width is constant along the rim. On the contrary, on the grafted layer (Figs. 1E–1N)

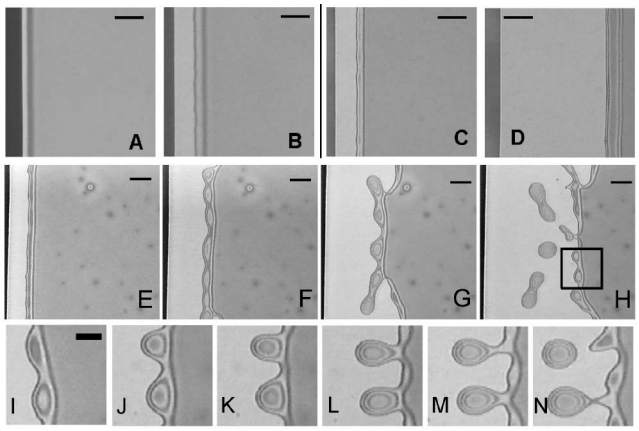

FIG. 1. Typical optical micrographs for the retraction of a thin PDMS film on a silicon wafer coated with a 6 nm adsorbed (images A–D) and a 6 nm grafted (images E–N) PDMS layer. The dewetted area appears lighter than the film. Retraction started at the edge of the sample shown on the left side of the frames. A–D: 24 nm PDMS (1000 Pa · s) at 130 °C for 80, 480, 1500, and 9900 sec, respectively. E–N: 50 nm PDMS (100 Pa · s) at 130 °C for 45, 110, 165, 245, 231, 258, 271, 287, 299, and 313 sec, respectively. The box indicated in frame H represents the area shown in frames I–N. Please note the fast moving dewetting front parallel to the initial rim in frames F–H. The frames in J–N are 3.0, 4.5, 8.5, 15.0, and 27.0 μm offset to the right with respect to image I. The length of the bar is 10 μm in A, B, I–N and 25 μm in C–H, respectively.

the rim started to undulate quite early, which eventually led to droplet formation. The undulations occurred at the front side of the rim while the rear side was still straight. An example for the formation of droplets is shown in Figs. 1I–1N. In contrast to fingering instabilities in driven systems where the front becomes wavy only normal to the pressure gradient [11–19] we observed dewetting in both directions, normal but also parallel to the rim. This occurred on the rear side of the initial rim where the width of the corresponding moving rim was comparatively small. As a consequence, the periodicity of the initial undulations was destroyed as seen in Fig. 1F, causing some polydispersity in droplet size.

As dewetting on grafted layers proceeded, rim instabilities led to continuous droplet formation in a somewhat irregular fashion (see Fig. 2). One can, however, clearly determine a straight line representing a mean dewetting front around which the local positions of the contact line fluctuate only by a small distance. The most surprising observation in our experiments is that the velocity V_{mean} of this mean front is *constant* (see Fig. 3B) although initially, as a consequence of slippage, the dewetting velocity was decreasing in time [22]. In the case of the adsorbed layer (see Fig. 3A) dewetting proceeded at an almost constant velocity, proving that there is no slip. Deviations from a constant velocity are expected as the assumption made by the approximate theory [27] that the front and the rear side of the rim move at the same speed is not fulfilled at early times.

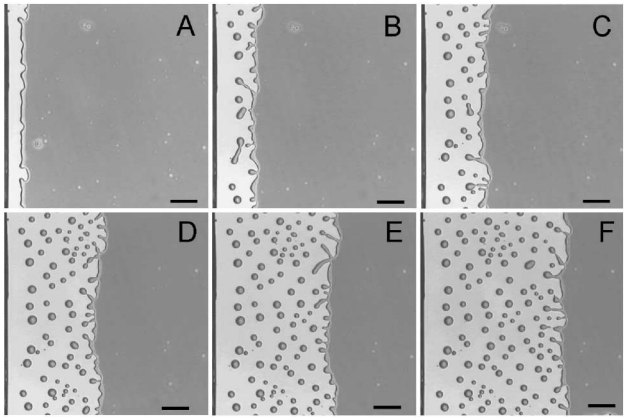

FIG. 2. Typical optical micrographs for the droplet formation at the later stages of the retraction of a 90 nm thin PDMS film (1000 Pa · s) at 130 °C on a silicon wafer coated with a 6 nm grafted PDMS layer for A: 60; B: 190; C: 310; D: 510; E: 690; and F: 870 sec, respectively. The length of the bar is 100 μm.

Both types of samples are almost identical. However, the adsorbed chains, containing loops and tails, resulted from a polydisperse and longer polymer than the densely end-grafted short polymers, causing different flow behaviors [20]. In our samples, the end-grafted polymers lose

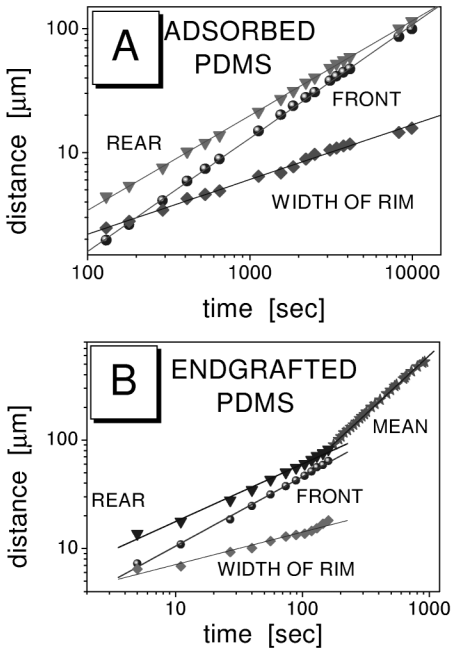

FIG. 3. Time (t) dependence of the displacement of the rim for the two samples shown in Fig. 1. For dewetting on an adsorbed PDMS layer (A) we found that the position of the front (F) and rear (R) side of the rim moved proportional to $t^{0.91\pm0.05}$ and $t^{0.76\pm0.05}$, respectively. The width (w) of the rim grew proportional to $t^{0.44\pm0.03}$. For the analogous system on the grafted layer (B), we found $F \sim t^{0.68\pm0.07}$ and $w \sim t^{0.33\pm0.03}$. The mean position of R—averaged over some 100 μm of length—was followed at later stages. It moved proportional to $t^{1.05\pm0.05}$, i.e., at an almost constant velocity. In contrast, at early times $R \sim t^{0.58\pm0.06}$ was found.

significantly more entropy than the adsorbed molecules due to the difference in Σ [23,26]. This, together with the tails and loops, is responsible for the difference in contact angle which was of the order of 1 deg for the adsorbed layers while it was of the order of 10 deg for the grafted layers [22]. In addition, the different chain conformations caused the slippage length to be about 10 μm for the grafted layer [22] and much smaller (probably zero) for the adsorbed layer [20]. We conclude that the no-slip boundary condition is obeyed on the adsorbed layer while slippage occurs on the brush (see Ref. [22]). Consequently, for the grafted layers, the friction force is proportional to the width of the rim, in contrast to being mainly determined by dissipation in the wedge close to the contact line [20,28].

Theoretically, the dewetting velocity V for nonslipping or slipping films is

$$V_{\text{no-slip}} = \frac{1}{6}\,\frac{\gamma}{\eta}\,\theta^2\,\frac{\theta}{L}\,, \tag{1}$$

$$V_{\text{slip}} = \frac{1}{6}\,\frac{\gamma}{\eta}\,\theta^2\,\frac{b}{w}\,, \tag{2}$$

with γ and η being the surface tension and the viscosity of the liquid, respectively, θ the contact angle the liquid forms on the substrate, L a constant of order 10 [1,28], b the slippage length, and w the width of the rim.

One can clearly see that $V_{\text{no-slip}}$ is constant while V_{slip} decreases in time as w increases, as observed in Fig. 3. Furthermore, for strong slippage and thin films V_{slip} will be much larger than $V_{\text{no-slip}}$. However, at late times, w could get larger than $w = bL/\theta$ and V_{slip} crosses over to $V_{\text{no-slip}}$ [20]. In our experiments we observed that V_{mean} was always larger than $V_{\text{no-slip}}$.

Using mass conservation [20,22] relating the dewetted area (Dh) with the cross section of the rim ($Cw^2\theta$) we can determine the "average" width of the rim at the onset of break-off of droplets ($w_{\text{break-off}}$):

$$w^2_{\text{break-off}} = \frac{D_{\text{mean}}\,h}{C\theta}\,. \tag{3}$$

Here, the constant $C = 0.1$ accounts for the asymmetric shape of the rim [20]. h is the film thickness. The mean dewetted distance (D_{mean}) between the resulting droplets (see Fig. 4A) increases about linearly with h and is also proportional to the wavelength of the fastest growing mode [3]. This observation is consistent with earlier results [2] where the diameter of the droplets as well as the distance between droplets were found to increase linearly with h in the case of unstable rims (on the so-called wafer B) [2].

The repeated, almost periodic, break-off of droplets hints that V_{mean} should be related to $w_{\text{break-off}}$. In fact, $V_{\text{mean}} \sim 1/w_{\text{break-off}} \sim 1/h$ (see Fig. 4B). In Fig. 4B, we have normalized V_{mean} according to Eq. (2) to account for differences in viscosity and contact angles between samples. Small differences in b have not been taken into account due to difficulties in determining b precisely enough [22].

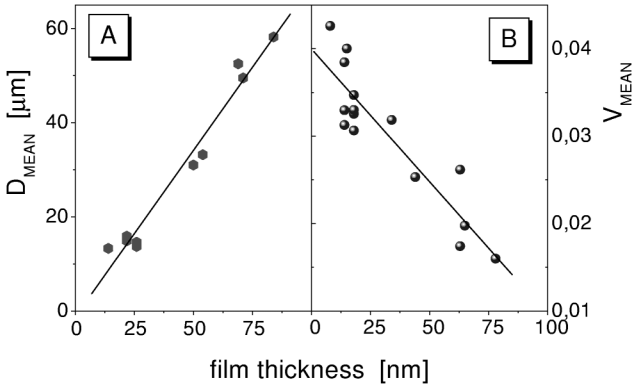

FIG. 4. Dependence of (A) D_{mean} and (B) V_{mean} — normalized by the capillary driving force and film viscosity, accounting for the different samples and temperatures used — on film thickness.

Finally, we note that the wavelength of the undulation pattern of the rim *before* droplet formation (Fig. 1F) is increasing in time (as the width of the rim grows) but also with film thickness. This is consistent with theoretical expectations [3] based on analogies to the Rayleigh instability. However, the same Rayleigh-like instability would be expected both for slipping and nonslipping films. From our experiments, we thus conclude that the initial small amplitude characteristic wavelength of the instability is likely set by the Rayleigh mechanism (minimization of the surface energy). However, an additional mechanism is needed for a rapid amplification of the instability leading to a visible, continuous formation and fragmentation of long fingers. Here, this mechanism is provided by the dependence of the dissipative term on the width of the rim, i.e., by a local increase (decrease) of the dewetting velocity with a local decrease (increase) in the rim width.

It may also be emphasized that we do not have a Marangoni type behavior as all interfacial tensions are constant. The dependence of the dewetting velocity on the width of the rim in the case of interfacial slippage is responsible for the spontaneous amplification of small fluctuations in the width of the rim. On the contrary, if the dewetting velocity is constant no instabilities of the rim are observed. Consequently, it is tempting to assume that rim instabilities imply that the films are slipping. This seems to be in accordance with previous experiments using polystyrene films on highly nonwettable substrates [2]. At present, the underlying physical mechanisms which lead to a *constant* "average" dewetting velocity are not yet fully understood. The self-regulation of the mean flow (the "base state") by the instability is a highly nonlinear, large amplitude phenomenon which cannot be investigated by the widely used linear stability analysis, since such an analysis assumes a base state independent of the instability. In some way this phenomenon is similar to the constant angle of repose of a sandpile. Continuously depositing sand onto the pile only

leads to fluctuations around this angle which is kept constant by avalanches [29]. In this sense, the phenomenon is also analogous to diffusion limited aggregation where the dendritic growth front proceeds at a constant velocity, but at the expense of instabilities [30]. One may call V_{mean} the self-regulated critical velocity of dewetting with slippage. We summarize that rim instabilities engender a constant and at the same time, much faster and thus highly efficient dewetting of the underlying substrate. As a general theme, nature seems to optimize the velocity of such kinetic processes by an appropriate self-modulation of the resulting structure.

We are indebted to Philippe Auroy for providing us with the endfunctionalized PDMS-molecules. The help of Rajesh Khanna with experiments is highly appreciated. Fruitful discussions with Françoise Brochard, Jean-François Joanny, and Jens-Uwe Sommer are gratefully acknowledged. This work was supported by the Indo-French Centre for the Promotion of Advanced Research/ Centre Franco-Indien Pour la Promotion de la Recherche.

[1] C. Redon, F. Brochard-Wyart, and F. Rondelez, Phys. Rev. Lett. **66**, 715 (1991).
[2] G. Reiter, Phys. Rev. Lett. **68**, 75 (1992); Langmuir **9**, 1344 (1993).
[3] F. Brochard-Wyart and C. Redon, Langmuir **8**, 2324 (1992).
[4] A. Sharma and G. Reiter, J. Colloid Interface Sci. **178**, 383 (1996).
[5] K. R. Shull and T. E. Karis, Langmuir **10**, 334 (1994).
[6] G. Debrégeas, P. Martin, and F. Brochard-Wyart, Phys. Rev. Lett. **75**, 3886 (1995).
[7] P. Lambooy, K. C. Phelan, O. Haugg, and G. Krausch, Phys. Rev. Lett. **76**, 1110 (1996).
[8] Q. Pan, K. I. Winey, H. H. Hu, and R. J. Composto, Langmuir **13**, 1758 (1997).
[9] R. Limary and P. F. Green, Langmuir **15**, 5617 (1999).
[10] C. Yuan, M. Ouyang, and J. T. Koberstein, Macromolecules **32**, 2329 (1999).
[11] F. Melo, J. F. Joanny, and S. Fauve, Phys. Rev. Lett. **63**, 1958 (1989).
[12] A. M. Cazabat, F. Heslot, S. M. Troian, and P. Carles, Nature (London) **346**, 824 (1990).
[13] J. B. Brzoska, F. Brochard-Wyart, and F. Rondelez, Europhys. Lett. **19**, 97 (1992).
[14] D. E. Kataoka and S. M. Troian, J. Colloid Interface Sci. **192**, 350 (1997).
[15] D. E. Kataoka and S. M. Troian, Nature (London) **402**, 794 (1999).
[16] S. M. Troian, E. Herbolzheimer, and S. A. Safran, Phys. Rev. Lett. **65**, 333 (1990).
[17] N. Samid-Merzel, S. G. Lipson, and D. S. Tannhauser, Phys. Rev. E **57**, 2906 (1998).
[18] K. R. Shull, C. M. Flanigan, and A. J. Crosby, Phys. Rev. Lett. **84**, 3057 (2000).
[19] A. Ghatak, M. K. Chaudhury, V. Shenoy, and A. Sharma, Phys. Rev. Lett. **85**, 4329 (2000).
[20] F. Brochard-Wyart, P. G. de Gennes, H. Hervert, and C. Redon, Langmuir **10**, 1566 (1994).
[21] C. Redon, J. B. Brzoska, and F. Brochard-Wyart, Macromolecules **27**, 468 (1994).
[22] G. Reiter and R. Khanna, Phys. Rev. Lett. **85**, 2753 (2000); Langmuir **16**, 6351 (2000).
[23] G. Reiter and R. Khanna, Phys. Rev. Lett. **85**, 5599 (2000).
[24] G. Reiter, R. Khanna, and A. Sharma, Phys. Rev. Lett. **85**, 1432 (2000).
[25] A. Casoli, M. Brendlé, J. Schultz, P. Auroy, and G. Reiter, Langmuir **17**, 388 (2001).
[26] L. Leibler, A. Ajdari, A. Mourran, G. Coulon, and D. Chatenay, in *Ordering in Macromolecular Systems,* edited by A. Teramoto, M. Kobayashi, and T. Norisuje (Springer-Verlag, Berlin, 1994), pp. 301–311.
[27] P. G. de Gennes, C.R. Seances Acad. Sci. Ser. II **303**, 1275 (1986).
[28] P. G. de Gennes, Rev. Mod. Phys. **57**, 827 (1985).
[29] D. L. Turcotte, Rep. Prog. Phys. **62**, 1377 (1999).
[30] E. Brener, H. Müller-Krumbhaar, and D. Temkin, Phys. Rev. E **54**, 2714 (1996).